We are IntechOpen, the world's leading publisher of Open Access books Built by scientists, for scientists

4,800
Open access books available

122,000
International authors and editors

135M
Downloads

Our authors are among the

154
Countries delivered to

TOP 1%
most cited scientists

12.2%
Contributors from top 500 universities

CLARIVATE ANALYTICS BOOK CITATION INDEX INDEXED

WEB OF SCIENCE™

Selection of our books indexed in the Book Citation Index in Web of Science™ Core Collection (BKCI)

Interested in publishing with us?
Contact book.department@intechopen.com

Numbers displayed above are based on latest data collected.
For more information visit www.intechopen.com

10

Preoperative Virtual Navigation with 3D-CT Volume Rendering for Single Minimum Incision Endoscopic Nephron-Sparing Surgery on Renal Tumors

Takao Kamai et al.*
Department of Urology, Tochigi
Japan

1. Introduction

Thanks to various technical and imaging innovations, pure laparoscopic or hand-assisted laparoscopic surgery is now performed worldwide and is considered to be safe and effective, while also improving the quality of life for patients [1,2]. However, laparoscopy requires three to four incisions, each of which is about 1-2 cm long. Every incision is associated with the potential risk of bleeding, hernia, and/or damage to internal organs, and also incrementally worsens the cosmetic outcome [3,4]. Furthermore, several problems remain to be solved with regard to laparoscopy, including the use of CO_2 pneumoperitoneum, the size of the incision required to retrieve the resected specimen, the need for trocar ports, and the high cost of equipment. Alternatives to conventional laparoscopy include single-site surgery, which is known as laparo-endoscopic single-site surgery (*LESS*), as well as natural orifice transluminal endoscopic surgery (NOTES). In 1998, Kihara *et al.* from Japan reported on minimum incision endoscopic surgery (MIES) performed via a single small incision, which was an attempt to solve the above-mentioned problems with conventional laparoscopic surgery and reduce technical difficulties (Figure 1) [5-9]. MIES is performed via a single small incision that is just large enough to allow extraction of the resected specimen, and is done without gas or trocar ports, making it a safe, reproducible, cost-effective, and minimally invasive treatment option [5-8].
Detection of small renal tumors has continued to increase as a result of improved imaging methods. In patients with a single, small (<4 cm), and localized renal cell carcinoma, nephron-sparing surgery (NSS) has become more common due to advances in renal imaging, improved surgical techniques, and the increasing number of incidentally discovered low-stage carcinomas. As a result, good tumor control and potentially better overall survival have been reported in patients undergoing NSS [10]. Therefore, radical nephrectomy is no longer the standard surgical procedure for such tumors and it has been

* Hideyuki Abe[1], Nobutaka Furuya[1], Tsunehito Kambara[1], Tomoya Mizuno[1], Daisuke Nishihara[1], Yasukazu Shioyama[2], Yoshitatsu Fukabori[1], Tomonori Yamanishi[1] and Yasushi Kaji[2]
[1]*Department of Urology, Tochigi,* [2]*Department of Radiology Dokkyo Medical University, Tochigi, Japan*

recognized that it could even be detrimental [10]. Although its safety is still controversial, use of laparoscopic NSS has been increasing [11]. Single MIES is based on both traditional open surgery and modified hand-assisted laparoscopic surgery [5], so the instruments employed are the same as those used for open or laparoscopic surgery and it only requires a short time to learn the technique [5-7]. Because MIES is performed via a small incision, however, the surgical field is very tight. Accordingly, extensive information about the renal tumor, renal vessels, and adjacent structures needs to be obtained preoperatively so that the surgeon can select the appropriate procedure. Moreover, the renal arteries and veins show anatomical variations that must be clarified before attempting surgical treatment, in order to reduce the risk of unexpected bleeding. It has been reported that CT scanning with three-dimensional (3D) reconstruction of images (3D-CT) and/or 3D-CT angiography (CTA) are useful modalities for viewing the renal arteries with less invasiveness than conventional angiography [12-14], and that these methods can be utilized for navigation when retroperitoneal laparoscopic nephrectomy is performed in patients with renal tumors [15]. We have employed preoperative 3D-CT for evaluation of the renal arteries and veins, as well as the relations between the renal hilar vessels and adjacent structures, in order to improve the outcome of single MIES nephrectomy [16], and have found that single MIES radical nephrectomy can be done more safely by utilizing 3D-CT images to perform virtual surgery, resulting in a shorter operating time and less blood loss.

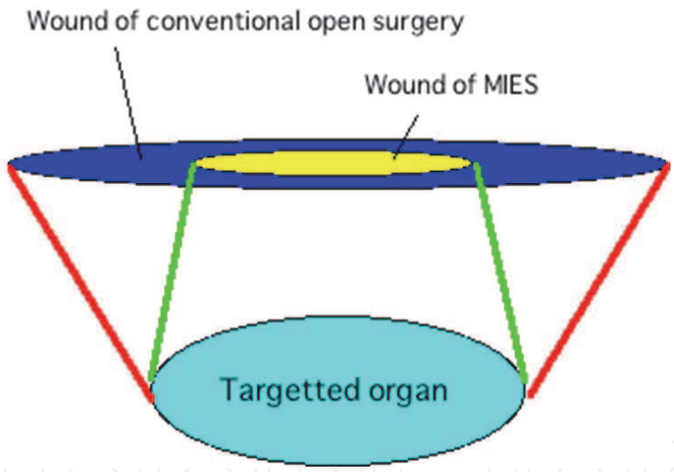

Fig. 1. Schema of single MIES. The length of the wound in MIES is 1/2 – 1/3 in open surgery.

In general, NSS is more difficult than radical nephrectomy and requires more preoperative anatomical data. In particular, detailed preoperative information on the relationship between the tumor and the renal vessels (arteries and veins) is important. It has been reported that 3D-CT provides superior images of the renal vessels and collecting system, and thus is useful for planning NSS [12,13,17]. The technique employed for single MIES nephrectomy of performing preoperative virtual surgery based on 3D-CT images reconstructed by the volume rendering method can also be used when NSS is done by single MIES [16].

In the present study, we reviewed the results of single MIES NSS for renal tumors in 50 consecutive patients treated by one chief operator (T.K*). We also assessed the usefulness of employing 3D-CT images for virtual surgery to decide the approach to the renal tumor during MIES NSS.

2. Methods

2.1 Patients

Fifty Japanese patients aged from 37 to 84 years (mean age: 58.1 years) with cT1aN0M0 renal tumors diagnosed between April 2003 and March 2011 underwent translumbar NSS by single MIES before receiving any other therapy. Patients with tumors located dorsally and very close to the renal hilar vessels were excluded, because such tumors are unsuitable for translumbar MIES. All patients underwent imaging (CT and/or MRI) prior to surgery in order to obtain information for staging. The tumor grade and clinical stage were assigned according to the Fuhrman grading system and the TNM classification, respectively [18,19]. Table 1 summarizes the demographic data, tumor location and size (on CT), operating time, and blood loss. The first 10 NSS procedures were performed without 3D-CT data and the subsequent 40 procedures were done after preoperative virtual surgery employing 3D-CT data. The operating time and blood loss in each group were analyzed in relation to tumor size, side, and location, as well as the length of the skin incision and the body mass index (BMI) [20]. This study was conducted in accordance with the Helsinki Declaration. Institutional Review Board approval was obtained and each patient signed a consent form approved by the Committee on Human Rights in Research of our institution.

	pre-operative axial CT (n = initial 10)	pre-operative 3D-CT (n = subsequent 40)	Surgical procedures (n = 50)
Patient demographics			
No. of patients	10	40	50
Age			58.3 (36 - 81)
Sex (male / female)			32 / 18
Tumor			
Tumor side (right / left)			26 / 24
Tumor size on CT (cm)		2.9 (1.5 - 8)	
MIES Operation			
Operative time (min)			116 (65 - 210)
Blood loss (ml)			212 (25 - 1000)

Table 1. Data collection from 3D-CT and surgical procedures

3. 3D-CT and preoperative virtual surgery

We usually perform NSS via the translumbar approach in patients with relatively small renal tumors. We did not obtain 3D-CT images for the initial 10 patients. However, 3D-CT was done in the subsequent 40 patients (who all had normal renal function and no allergy to contrast medium) in order to plan an appropriate and safe approach to the renal arteries and veins [9]. All of the axial scans (obtained by multidetector row CT) were carefully evaluated before 3D reconstruction was performed, and then 3D images were created by software built into the CT scanner (Leonardo InSpace, Siemens Healthcare, Forchheim, Germany). The arterial phase was used to depict both the renal arteries and veins, since it is the most

sensitive phase for the detection of multiple vessels as well as other abnormalities [21]. Data from the CT scans were employed to construct 3D images, after which virtual surgery was performed on a computer. Using the 3D images, the location of the kidney in relation to the lower ribs, iliac crest, and spine was determined to help the surgeon select the best site for making the incision. Possible involvement of adjacent structures by the tumor was also investigated. Images were created that gave an oblique view from the skin incision to the targeted renal artery and vein, in order to allow the surgeon to better understand the anatomical relations between the renal hilar vessels and the surrounding structures. The software (Leonardo InSpace or public domain software OsiriX) allowed the kidney to be freely rotated into different positions and facilitated the creation of any desired cut plane, so that relations between the tumor and the renal vessels or adjacent structures could be demonstrated clearly. Virtual surgery was started by making an oblique intercostal incision between the 11 and 12th ribs. After dissecting between the psoas muscle and Gerota's posterior fascia, we approached the kidney anterior to the psoas muscle. On the right side, we found the posterior surface of the inferior vena cava (IVC) behind the psoas muscle at the level of the lower pole of the kidney. Then we advanced along the IVC toward the liver and identified the right renal artery (RRA). At this level, we also found the right renal vein (RRV) branching from the right side of the IVC. When operating on the left kidney, we initially identified the left renal artery (LRA) running vertical to the psoas muscle at the midpoint of the kidney, after which we identified the left renal vein (LRV) lying behind (ventral to) the LRA. We usually performed simulated surgery from the dorsal to ventral direction as in actual surgery, but we also assessed oblique images in the opposite (ventral to dorsal) direction to better understand relations between the renal vessels and the tumor or adjacent structures.

Because we do not clamp the renal artery for NSS if possible, we need to pay close attention to information about the renal vessels near the tumor in order to preserve renal function. Thus, the renal arteries and veins were followed toward the tumor in order to detect the arterial branches feeding the lesions and the veins draining it (Figure 2 to 5).

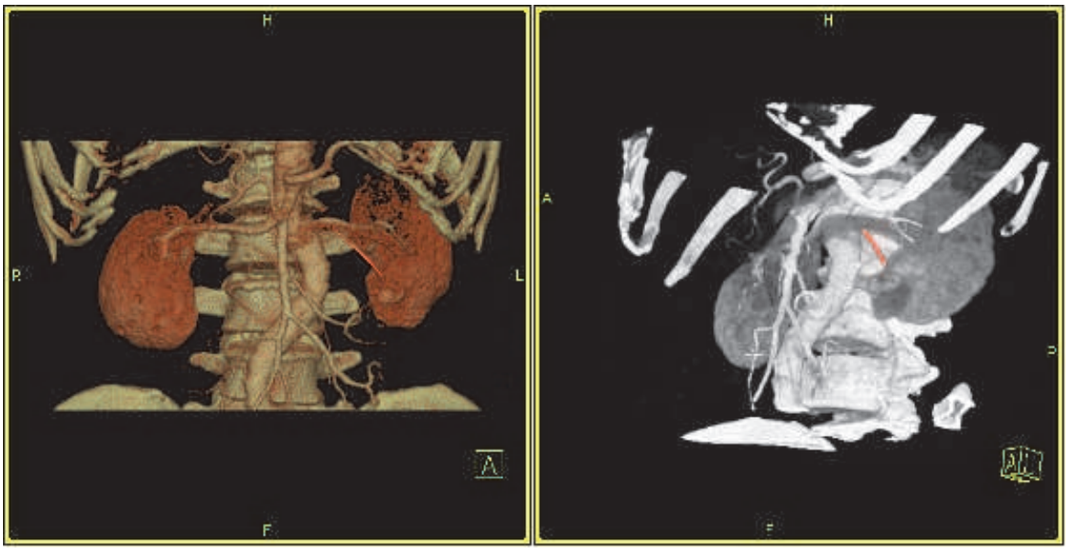

Fig. 2. A left renal tumor. Anterior view (left) and oblique view (right) in the arterial phase. The tumor is located in the ventral lower pole of the kidney. An artery (red) branches off from a proximal vessel and runs toward the tumor. This is the feeding artery.

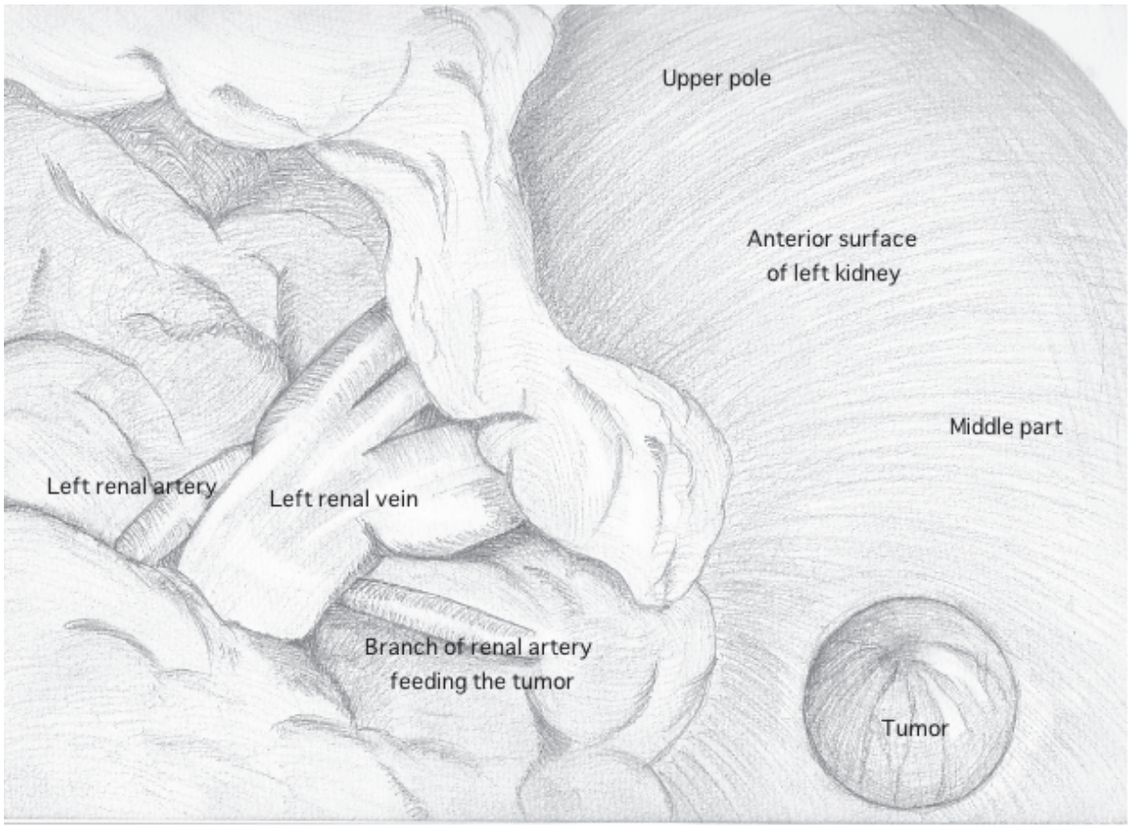

Fig. 3. Sketches of the surgical field viewed through the narrow incision in the Figure 2 for MIES NSS. The tumor is located in the ventral lower pole of the kidney. After dissection between the peritoneum and Gerota's anterior fascia, Gerota's fascia was bluntly dissected to access the renal hilum and the tumor.

4. Surgical technique

We performed NSS by single MIES via the translumbar approach with the patient in the flank position over the break of the operating table according to the reported method [16]. The surgical team consisted of the chief operator and two or three assistants. A flexible high-definition laparoscope (Olympus, Tokyo, Japan) was manipulated by one of the assistants and was moved to the best position for viewing the operating field. The chief operator and first assistant employed a combination of video images and direct vision, while only video images were available for the other assistants.

Based on 3D treatment planning, an oblique intercostal skin incision was made between the 11 and 12th ribs with an average length of about 5 cm (4-6), and a wound retractor (2.5-6 cm in diameter, Applied Medical, CA) was attached. After the external and internal oblique muscles were split, the transversalis fascia was incised, and dissection was performed between the psoas fascia and Gerota's posterior fascia to approach the kidney anterior to the psoas muscle. Gerota's posterior fascia was bluntly dissected and pushed medial to the psoas muscle, achieving immediate access to the renal arteries and veins. We identified the renal artery and vein by manipulation as described previously [16].

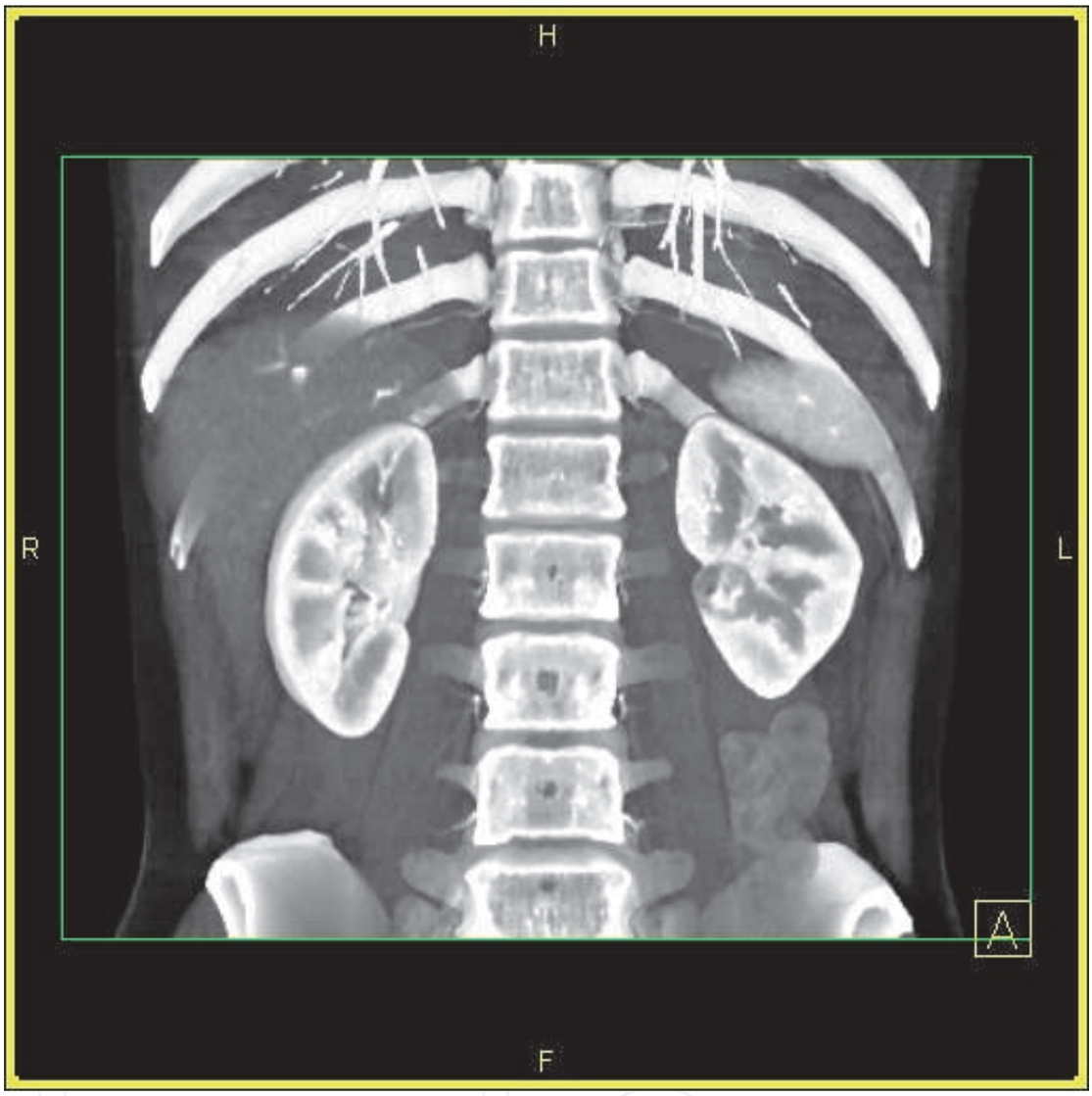

Fig. 4. A left renal tumor adjacent to the renal artery and vein.

After dissecting between the psoas fascia and Gerota's posterior fascia to approach the posterior (dorsal) surface of the kidney, dissection was performed between the peritoneum and Gerota's anterior fascia to approach the anterior (ventral) surface of the kidney. Dissecting both sides of the kidney was useful for mobilization and for approaching the tumor. Gerota's posterior fascia was bluntly dissected and pushed medial to the psoas muscle, achieving access to the renal vessels. Then Gerota's fascia covering the tumor was exposed. We used ultrasonography to find smaller tumors, if necessary. Next, Gerota's fascia was cut close to the tumor and the perinephric fat was dissected to approach the normal renal parenchyma near the lesion. If the tumor was on the posterior (dorsal) side, Gerota's posterior fascia was bluntly pushed medially off the psoas muscle, and the renal pedicle was exposed via the posterior approach. When the tumor was on the anterior (ventral) side, Gerota's anterior fascia was bluntly pushed laterally off the peritoneum and the renal pedicle was exposed via the anterior approach. Microwave tissue coagulation was

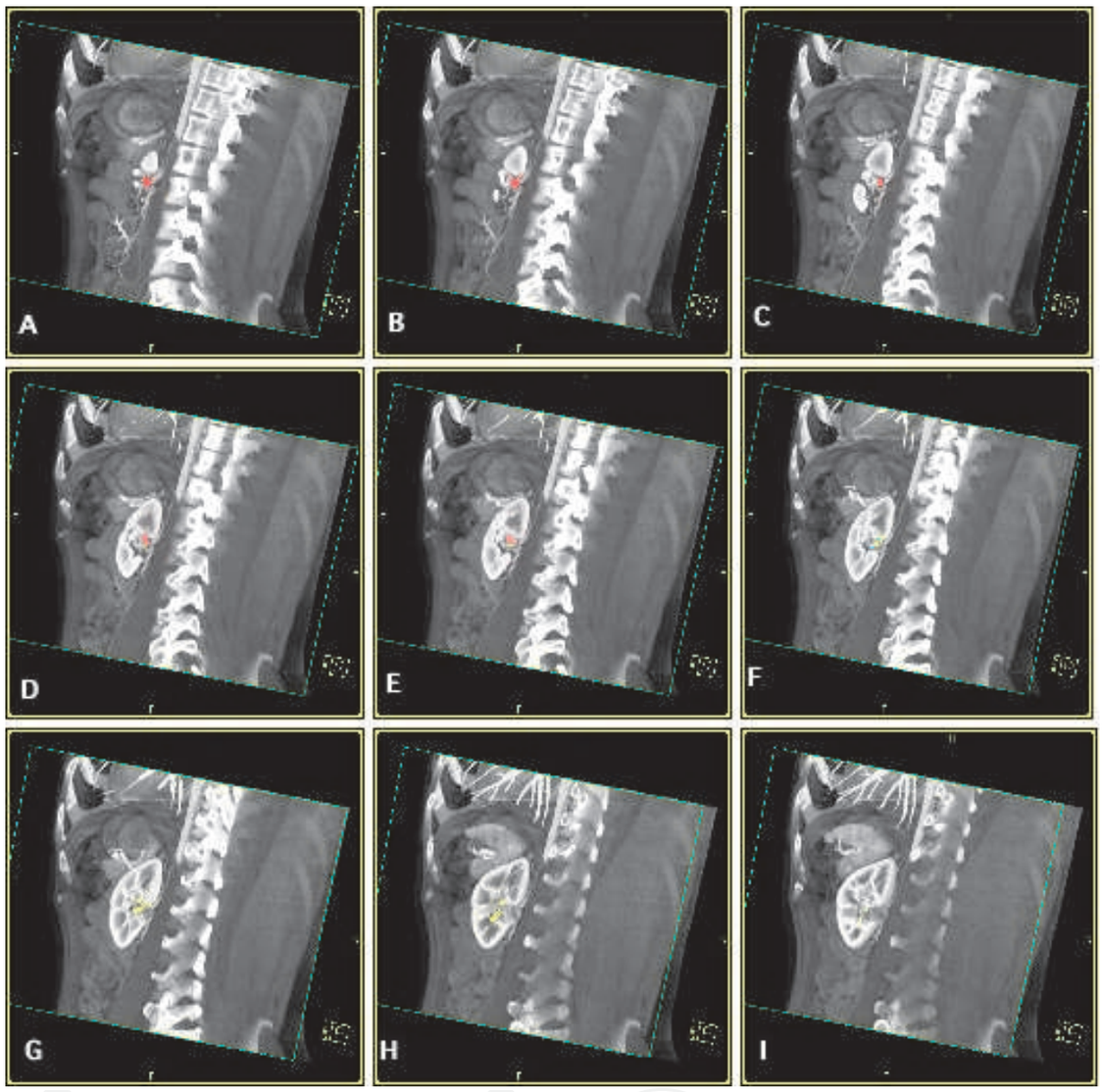

Fig. 5. A left renal tumor very close to the renal hilum (Figure 3). Oblique view from the dorsal to ventral direction in the arterial phase. The CT scans are arranged from central (A) to lateral (I). A, B, C: An artery (red) branches off from a proximal vessel and run toward the periphery. D, E: The artery (red) divides into three small arteries (red, red, and yellow). F: The yellow artery divides into four arterioles (two yellow and two blue). G, H, I: The tumor can be seen in the midportion of the kidney. Two yellow arteries run close to the tumor (T) with a branching artery (green). During NSS, we should pay careful attention to this yellow artery that may feed the tumor.

performed with a Microtaze OT-110 M microwave generator and a needle-type monopolar electrode that was 1.0 to 1.5 cm long and 1 mm in diameter. Coagulation with the electrode was done at 0.5 to 1 cm from the tumor margin. The electrode was inserted into the renal parenchyma at 5 to 10 mm intervals for coagulation at 50 W for 45 seconds, followed by 15 seconds of rest. If the tumor was located close to the renal pedicle, coagulation of the parenchyma was limited to avoid injury to the renal artery or vein and the tumor was

excised with scissors or a harmonic scalpel by cutting along the middle of the coagulated zone. The renal artery was clamped, if necessary. After transected vessels were ligated and the collecting system was sutured, indigocarmine was injected intravenously to confirm that there was no significant leakage of urine. An argon beam coagulator was applied to achieve complete hemostasis of the cut surface, if required. All renal defects were filled with perinephric fat and the resected tumor was retrieved thorough the incision. After placing a drain tube within Gerota's fascia, the skin was closed.

5. Statistical analysis

Since the data did not show a normal distribution, the results were analyzed by employing the non-parametric Mann-Whitney *U* test for comparison between two groups and the non-parametric Kruskal-Wallis test to compare three groups. Because Boneferroni's correction is generally employed for multiple comparisons, the Mann-Whitney *U* test was corrected by this method. A probability (P) value of less than 0.05 was considered significant. Analyses were done with commercially available software.

6. Results

NSS was performed successfully by single MIES in all 50 patients. The baseline demographic, clinicopathological, intraoperative, and postoperative data of the subjects are summarized in Table 2. Although there were no operative complications, the incision was extended by 1 to 2 cm in three patients to control hemorrhage. Bleeding was successfully arrested in all three patients and none of them required blood transfusion.

Preoperative 3D reconstruction of volume-rendered images was done in 40 patients, but the first 10 procedures were performed without 3D-CT data. The 50 patients were divided into three groups. There were no differences of tumor size among the groups (data not shown). The operating time (mean ± S.D.) for the initial 10 NSS performed without virtual surgery was 141.9±40.7 min, and there was a significant decrease in the second (117.9±25.7 min, P=0.0440) and third (102.36±19.4 min, P=0.0024) groups that received NSS after preoperative virtual surgery (Figure 6A). Furthermore, the operating time in third group was shorter than in second group (P=0.0353). In contrast, there was tendency toward smaller blood loss in the second group (192.4±110.2 ml) and the third group (191.5±103.2 ml) than in the first group (303.1±291.5 ml), but there was no statistical difference (Figure 6B). There were no differences between tumors on the right and left sides with regard to the operating time (data not shown) or blood loss (data not shown).

We also analyzed the influence of tumor size and location on the operating time and blood loss. Tumors that were located at the upper pole (132.4±34.2 min) and middle part (115.3±33.8 min) required a longer operation time than those at the lower pole (132.4±34.2 min, P=0.0323, Figure 6C). Similarly, tumors that were located at the lower pole (154.0±57.2 ml, P=0.0037) had a smaller blood loss than those at the upper pole (311.2±216.0 ml) and middle part (193.5±145.9 ml, Figure 6D).

There was no difference of the operating time between the ventral side (118.9±34.0 min) and the dorsal side (110.6±15.7 min, P=0.3602, Figure 6E), and but the blood loss of the ventral side (193.9±174.4 ml) was smaller than those of the dorsal side (243.9±115.1 ml, P=0.0347, Figure 6F).

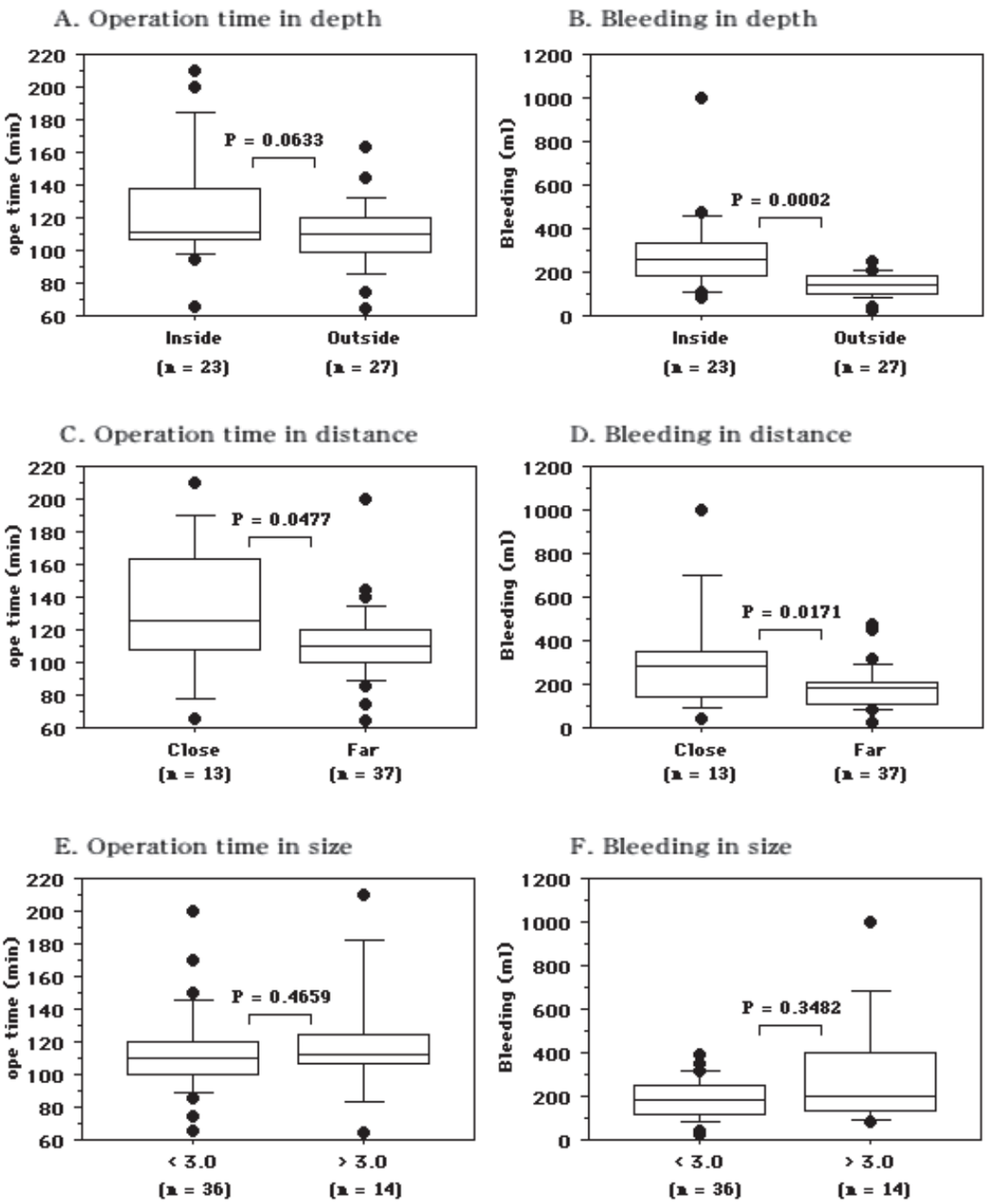

Fig. 6. Comparison of the first to third NSS groups with regard to operating time (A), blood loss (B). Comparison of tumor location between patients with lower pole, middle part, upper pole, dorsal (Dor), and ventral (Ven). Median values are shown in the box plots. Bold circled P values were obtained by comparing the three groups with the Kruskal-Wallis test.

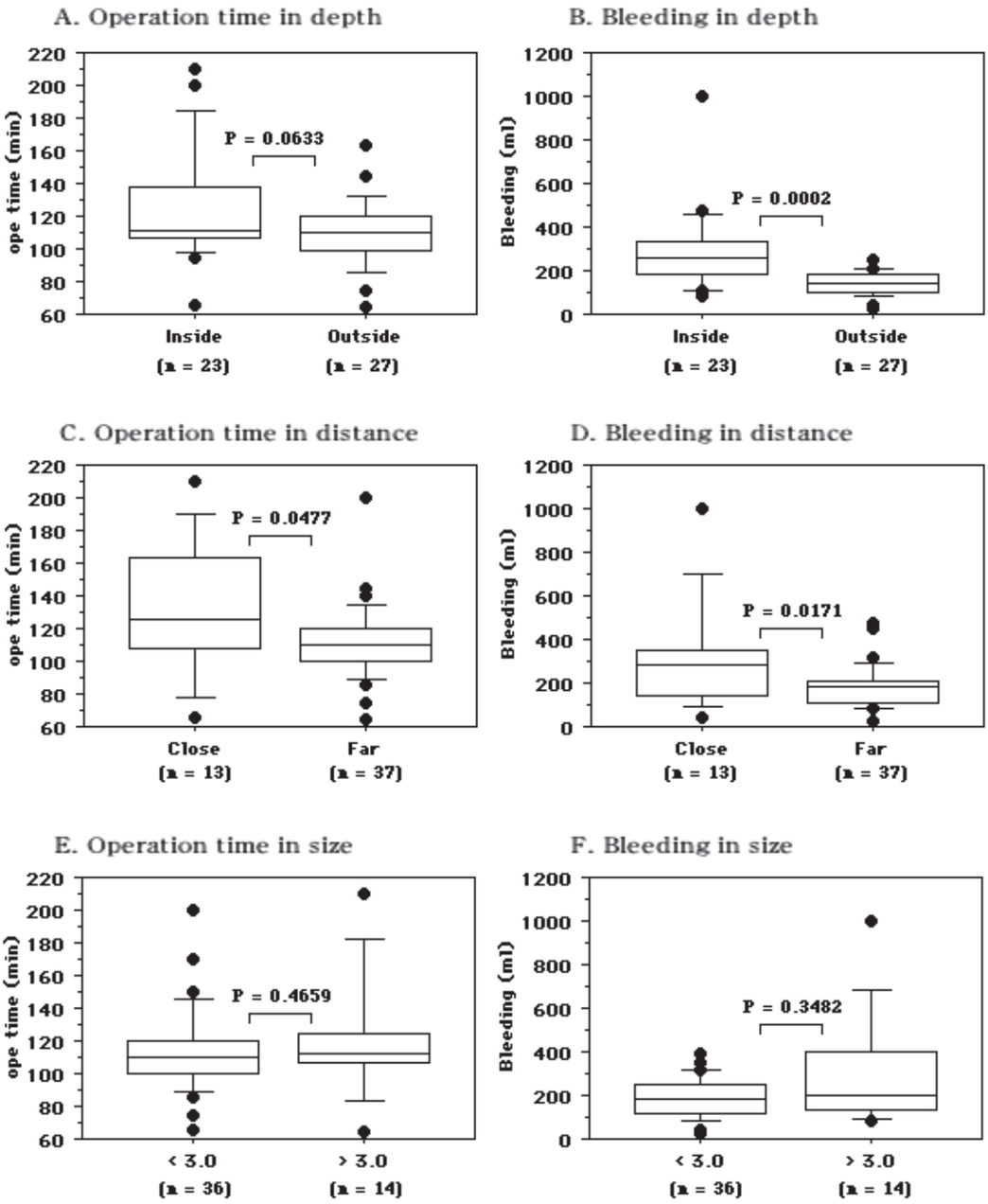

Fig. 7. Operating time and bleeding in relation to tumor location and size. A,B: Tumor depth. Equator of tumor was below (Inside) and above (Outside) the kidney surface. C,D: Tumor is close to (Close) or far from the renal hilum (Far). E,F: Tumor smaller or larger than 3 cm in diameter.

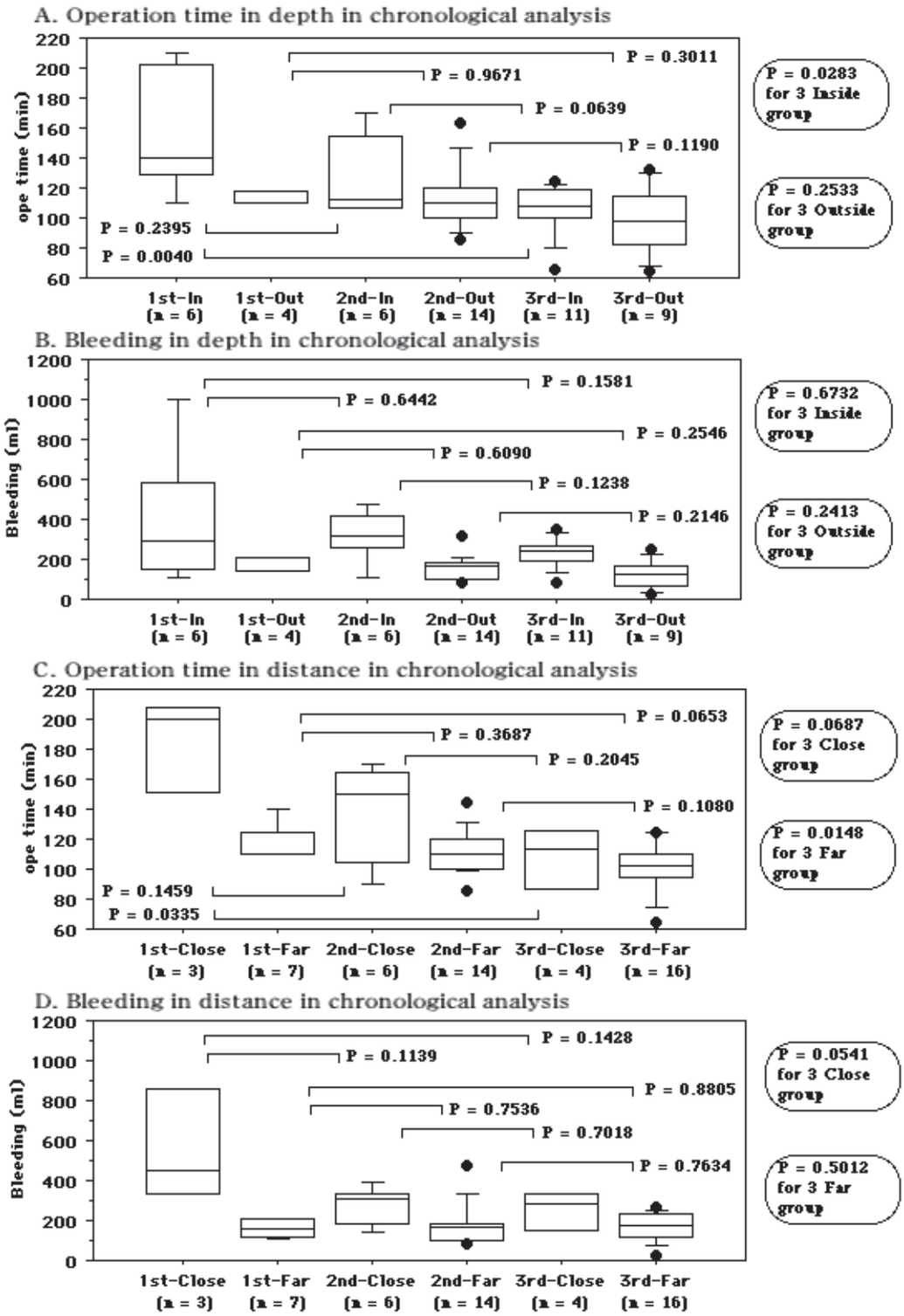

Fig. 8. Comparison of operating time and bleeding in relation to tumor depth (Inside or Outside) and distance (Close or Far) between the first to third NSS groups. Bold circled P values were obtained by comparing the three groups with the Kruskal-Wallis test.

The tumors that were relatively deeply (inside) located required longer operation time and larger blood loss (124.9±34.9 min, 296.8±197.8 ml) than those relatively superficially (outside) located (108.8±21.1 min, *P*=0.0633; 143.6±54.7 ml, *P*=0.0002, Figure 7A,B)
Tumors that were located close to renal hilum required a longer operation time (131.8±42.4 min) and a greater blood loss (314.1±264.8 ml) than those far from hilum (111.4±22.6 min, *P*=0.0477; 182.5±95.5 ml, *P*=0.0171, Figure 7C,D).
There were no difference of the operating time and blood loss between tumor size (Figure 7E,F).
In the chronological analysis, the operating time in the tumor that was inside (Figure 8A) and far from the hilum (Figure 8C) was dramatically shorter when the procedure was done after preoperative virtual surgery than when it was done without simulation. There was also shorter operating time and less blood loss in the tumor close to the hilum when NSS was done after virtual surgery (Figure 8C,D).

7. Discussion

Since we were familiar with the anatomical frame, landmarks, and operating technique for radical nephrectomy of cT1-3aN0M0 renal tumors via the translumbar approach, we also employed this approach for NSS by single MIES. The present results demonstrate that NSS can be performed safely by single MIES. The extraperitoneal subcostal translumbar approach avoids the risk of peritoneal contamination and also results in earlier resumption of normal bowel function after surgery. We used 3D-CT images to display the location of the kidney in relation to the lower rib cage, iliac crest, and spine, thereby helping the surgeon to accurately plan the initial incision. The position of the kidney and the location and size of the tumor determined the length of the incision.
Preoperative 3D imaging of the renal arteries and veins has been reported to provide useful information for laparoscopic nephrectomy [15,16]. Single MIES is performed via a single small incision, so detailed anatomical information is required in order to approach the renal artery and vein safely as the operation progresses step-by-step with manipulation of the endoscope and instruments in the narrow surgical field. We performed preoperative CT and used the volume rendering method for reconstruction of 3D images because it retains all data by summing the contributions from each voxel along a line set at any viewing angle through a stack of axial images. After 3D images are created, two-dimensional images can also be obtained. Thus, the 3D-CT images can be employed to view the kidney in different positions and 2-dimensional images can be created in any desired plane for clear demonstration of the relations between the tumor and the renal vessels or adjacent structures. In addition, performing virtual surgery is likely to provide the surgeon with more information than that gained from careful study of standard axial CT scans.
We think that the most important point for NSS is to avoid damage to the renal arteries and veins, particularly when the tumor is close to the hilar vessels (Figure 7). It is also difficult to manipulate the tumors whose equator was below (Inside) the kidney surface (Figure 7). Resection of upper pole tumors took longer and was associated with more blood loss (Figure 6).
Comparison between our first 10 NSS procedures and the subsequent 40 with preoperative virtual surgery revealed that latter group had a shorter operating time and smaller blood loss in the tumors whose equator was below (Inside) the kidney surface or close to the renal hilum (Figure 8). Based on data from preoperative 3D simulation, intraoperative experience,

and re-evaluation of our surgical technique by reviewing operative videos for the subsequent 40 patients, we have developed a successful method for approaching the tumor and handling the feeding artery and the hilar vessels. As described in Methods, our approach to the feeding artery and hilar vessels was improved by review of 3D-CT information. These results may reflect both the feedback effect and the learning curve related to accumulation of experience with virtual surgery and actual NSS, indicating that virtual surgery based on 3D-CT data is useful for identifying the feeding artery and renal hilar vessels and for assessing their relations to the tumor, allowing NSS to be performed more safely by single MIES. However, a randomized trial comparing the outcome of patients with or without preoperative virtual surgery should be performed in order to confirm that simulation based on 3D-CT images is useful.

Single MIES is based on standard open surgery, but we use a flexible high-definition laparoscope for easy identification of tissue planes and to allow more precise dissection with minimal trauma. Many of the longer instruments used in open surgery can be inserted into the narrow incision for MIES, so it has a lower cost than conventional laparoscopic surgery (30-40% less). Moreover, the assistants at our hospital are now performing single MIES as chief operators. Because of their experience with this technique, including direct vision and viewing video images as assistants during many single MIES procedures, they had a relatively short learning period. Another advantage of single MIES is that the incision can be extended quickly if required.

Since we have no experience of *LESS* or NOTES, we could not determine whether or not those procedures are superior to single MIES for NSS. However, any of these new single-site laparo-endoscopic procedures and robotic-assisted methods may be a potential alternative to conventional open or laparoscopic surgery.

8. Acknowledgement

The authors are grateful to Junka for her excellent sketches of the surgical field, and Kazumoto Kimura, PhD, for his constructive suggestions regarding statistical analysis.

9. Conclusion

NSS can be performed more safely by single MIES after utilizing 3D-CT images to carry out preoperative virtual surgery, resulting in a shorter operating time and less blood loss.

10. References

Dunn MD, Portis AJ, Shalhav AL, Elbahnasy AM, Heidorn C, McDougall EM, Clayman RV : Laparoscopic versus open radical nephrectomy: a 9-year experience. *J Urol* 2000, 164 : 1153-1159.

Rassweiler J, Frede T, Henkel TO, Stock C, Alken P : Nephrectomy: a comparative study between the transperitoneal and retroperitoneal laparoscopic versus the open approach. *Eur Urol* 1998, 33 : 489-496.

Raman JD, Cadeddu JA, Rao P, Rane A : Single-incision laparoscopic surgery: initial urological experience and comparison with natural-orifice transluminal endoscopic surgery. *BJU Int* 2008, 101 : 1493-1496.

Kommu S, Kaouk JH, Rane A. Laparo-endoscopic single-site surgery; preliminary advances in renal surgery. *BJU Int* 2008, 103 : 1034-1037.

Kihara K, Kawakami S, Fujii Y, Masuda H, Koga F : Gasless single port access endoscopic surgery in urology: Minimum incision endoscopic surgery, MIES. *Int J Urol* 2009, 16 : 791-800.

Kihara K, Kageyama Y, Yano M, Kobayashi T, Kawakami S, Fujii Y, Masuda H, Hyochi N : Portless endoscopic radical nephrectomy via a single minimum incision in 80 patients. *Int J Urol* 2004, 11 : 714-720.

Kageyama Y, Kihara K, Ishizaka K, Okuno T, Hayashi T, Kawakami S, Masuda H, Suzuki M, Hyochi N, Arai G : Endoscopic minilaparotomy radical nephrectomy for chronic dialysis patients. *Int J Urol*, 2002, 9 : 73-76.

Kageyama Y, Kihara K, Kobayashi T, Kawakami S, Fujii Y, Masuda H, Yano M, Hyochi N Portless endoscopic adrenalectomy via a single minimum incision using a retroperitoneal approach: Experience with initial 30 cases. *Int J Urol* 2004, 11 : 693-699.

Kamai T, Yoshida K : Portless endoscopic radical nephrectomy. *Urology View,* Tokyo, 2006, 4 : 66-72.

Novick AC : Open surgery of the kidney. In Wein AJ, Kavoussi LR, Novick AC, Partin AW, Peters CA., editors. Campbell-Walsh Urology. 9th Edition. Philadelphia: Saunders Elsevier; 2007. P.1686-1758.

Gill IS, Kamoi K, Aron M, Desai MM. 800 laparoscopic partial nephrectomies: a single surgeon series. *J Urol* 2010, 183 : 34-41.

Chernoff DM, Silverman SG, Kikinis R, Adams DF, Seltzer SE, Richie JP, Loughlin KR : Three dimensional omaging and display of renal tumors using spiral CT; a potential aid to partial nephrectomy. *Urololgy* 1994, 43 : 125-129.

Coll DM, Uzzo RG, Herts BR, Davros WJ, Wirth SL, NOVICK AC : 3-Dimensional volume rendered computerized tomography for preoperative evaluation and intraoperative treatment of patients undergoing nephron sparing surgery. *J Urol* 1999, 161 : 1097-1102.

Coll DM, Herts BR, Davros WJ, Uzzo RG, Novick AC : Preoperative use of 3D volume rendering to demonstrate renal tumors and renal anatomy. *Radiographics* 2000, 20 : 431-438.

Marukawa K, Horiguchi J, Shigeta M, Nakamoto T, Usui T, Ito K : Three-dimensional navigator for retroperitoneal laparoscopic nephrectomy using multidetector row computerized tomography. *J Urol* 2002, 168 : 1933-1936.

Kamai T, furuya N, Kambara T, Abe H, Honda M, Shioyama Y, Kaji Y, Yoshida K : Single minimum incision endoscopic radical nephrectomy for renal tumors with preoperative virtual navigation using 3D-CT volume-rendering. *BMC Urology*, 2010, 10: 1471-2490-10-7.

Ueda T, Tobe T, Yamanoto S, Motoori K, Murakami Y, Igarashi T, Ito H : Selective intra-arterial 3-dimensional computed tomography angiography for preoperative evaluation of nephron-sparing surgery. *J Comput Assist Tomogr* 2004, 28 : 496-504.

Fuhrman SA, Lasky LC, Lmas C : Prognostic significance of morphologic parameters in renal cell carcinoma. *Am J Surg Pathol* 1982, 6 : 655-663.

Sobin LH, Wittekind CH editors. : International union against cancer. UICC, *In* TNM classification of malignant tumors, 6rd ed. New York, Wiley-Liss, 2002.

WHO. Obesity: preventing and managing the global epidemic. Report of a WHO Consultation. WHO Technical Report Series 894. Geneva: World Health Organization. 2000.

Herts BR, Coll DM, Lieber ML Streem SB, Novick AC : Triphasic helical CT of the kidneys: contribution of vascular phase scanning in patients before urologic surgery. *Am J Roentgenol* 1999, 173 : 1273-1277.

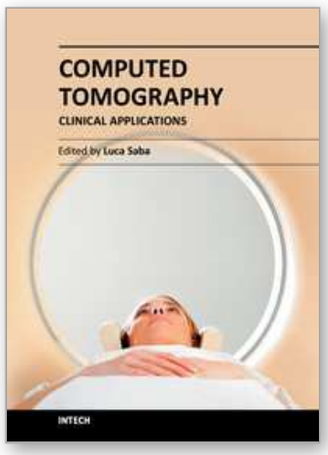

Computed Tomography - Clinical Applications
Edited by Dr. Luca Saba

ISBN 978-953-307-378-1
Hard cover, 342 pages
Publisher InTech
Published online 05, January, 2012
Published in print edition January, 2012

Computed Tomography (CT), and in particular multi-detector-row computed tomography (MDCT), is a powerful non-invasive imaging tool with a number of advantages over the others non- invasive imaging techniques. CT has evolved into an indispensable imaging method in clinical routine. It was the first method to non-invasively acquire images of the inside of the human body that were not biased by superimposition of distinct anatomical structures. The first generation of CT scanners developed in the 1970s and numerous innovations have improved the utility and application field of the CT, such as the introduction of helical systems that allowed the development of the "volumetric CT" concept. In this book we want to explore the applications of CT from medical imaging to other fields like physics, archeology and computer aided diagnosis. Recently interesting technical, anthropomorphic, forensic and archeological as well as paleontological applications of computed tomography have been developed. These applications further strengthen the method as a generic diagnostic tool for non- destructive material testing and three-dimensional visualization beyond its medical use.

How to reference
In order to correctly reference this scholarly work, feel free to copy and paste the following:

Takao Kamai, Hideyuki Abe, Nobutaka Furuya, Tsunehito Kambara, Tomoya Mizuno, Daisuke Nishihara, Yasukazu Shioyama, Yoshitatsu Fukabori, Tomonori Yamanishi and Yasushi Kaji (2012). Preoperative Virtual Navigation with 3D-CT Volume Rendering for Single Minimum Incision Endoscopic Nephron-Sparing Surgery on Renal Tumors, Computed Tomography - Clinical Applications, Dr. Luca Saba (Ed.), ISBN: 978-953-307-378-1, InTech, Available from: http://www.intechopen.com/books/computed-tomography-clinical-applications/preoperative-virtual-navigation-with-3d-ct-volume-rendering-for-single-minimum-incision-endoscopic-n

INTECH
open science | open minds

InTech Europe
University Campus STeP Ri
Slavka Krautzeka 83/A
51000 Rijeka, Croatia
Phone: +385 (51) 770 447
Fax: +385 (51) 686 166
www.intechopen.com

InTech China
Unit 405, Office Block, Hotel Equatorial Shanghai
No.65, Yan An Road (West), Shanghai, 200040, China
中国上海市延安西路65号上海国际贵都大饭店办公楼405单元
Phone: +86-21-62489820
Fax: +86-21-62489821

IntechOpen